Electronic Supplementary Material (ESI) for Reaction Chemistry & Engineering.

Adaptive and automated system-optimization for heterogeneous flow-hydrogenation reactions

David C. Fabry, Steffen Heddrich, Erli Sugiono,* Marcel A. Liauw,* und Magnus Rueping*

Magnus.rueping@rwth-aachen.de

Experimental Setup: H-Cube (step size), HPLC Pump Knauer K-120 (Dr. Ing. Herbert Knauer GmbH)[1], autosampler AutoSam200 (HiTec Zhang GmbH)[2] and Upchurch Scientific (IDEX Health & Science LLC)[3] connectors.

The catalyst cartridges were manually packed and loaded with 0.307 g 5 wt.-% Pd/C (E101 O/W) from Evonik Degussa or 0.278 / 0.255 g 2.5/10 wt.-% Ir@CNT. The cardiges were used over the entire course of the respective optimizations and not exchanged or refilled.

Optimization of 2: c(benzaldehyde 2 in 1L MeCN) = 0.25 M, parameter limits for H_2 pressure 10 – 100 bar, flow rate 0.3 – 1.0 mL min^{-1}, temperature 20 – 100 °C, starting values 0.5 mL min^{-1}, 40 °C, 20 bar H_2 pressure.

Optimization for 3: c(ethylphenyl glyoxylate 3 in 0.5 L MeCN) = 0.15 M, parameter limits for H_2 pressure 10 – 100 bar, flow rates 0.3 – 1.0 mL min^{-1}, temperature 20 – 75 °C, starting values 0.7 mL min^{-1}, 30 °C, 10 bar H_2 pressure.

Optimization for 5: c(quinaldine 5 in 0.1 L EtOAc) = 0.10 M, parameter limits for H_2 pressure 10 – 100 bar, flow rates 0.3 – 1.0 mL min^{-1}, temperature 20 – 75 °C, starting values 0.7 mL min^{-1}, 30 °C, 10 bar H_2 pressure.

Optimization for 5: c(quinaldine 7 in 0.1 L EtOAc) = 0.10 M, parameter limits for H_2 pressure 10 – 100 bar, flow rates 0.3 – 1.0 mL min^{-1}, temperature 20 – 75 °C, starting values 0.7 mL min^{-1}, 30 °C, 10 bar H_2 pressure.

Products were characterized either by NMR or GC with calibration and compared to commercially available samples.

MSIM-algorithm implemented as Matlab 7 plug-in to LabView 2010 based on [4]; H-Cube, valve and autosampler controlled by LabView 2010 via serial RS-232 connections.

$$P_i = P1 + q + \frac{c}{\sqrt{2}} \cdot E_{i-1}$$

$$q = \frac{c \cdot \left(\sqrt{d+1} - 1\right)}{d \cdot \sqrt{2}} \cdot a$$

P1	starting point (vector: flow rate/temperature/pressure)
P_i	other points of starting tetragon (i = 2 – 4)
c	edge length (0.3)
a	corrector value [25 1 0.75]
d	dimension (3 - flow rate, temperature, pressure)
E	unit matrix (*d* x *d*)

Starting values were chosen within parameter ranges that formed a suitably large starting tetragon from which further optimization can be initiated (Table S1). The starting tetragon was created with one starting point *P1* and an edge length *c* based on a method of Spendley *et al.*.[5] All points which were generated by the MSIM-algorithm were rounded to the nearest step size value of the HCube (flow rate in 0.1 $mLmin^{-1}$ steps, temperature in 5 K steps and pressure in 10 bar steps).

Description of flow setup and water electrolysis

The integrated electrolysis cell enables the electrochemical formation of hydrogen from deionized water avoiding the hazards associated with handling large quantities of hydrogen. The hydrogen formed is subsequently fed via a mixer into the substrate-solvent flow. By installing different heterogeneous catalysts the system provides scope for a wide spectrum of hydrogenations to be performed. Furthermore, by utilizing the integrated heating block and the backpressure valve reactions can be performed at temperatures as high as 100°C and pressures up to 100 bar. Hydrogen is generated and mixed automatically in the commercially available H-Cube. The pressure value given for hydrogen corresponds to the pressure generated inside the H-Cube and applied to the catalyst chamber. Pressure regulators at the apparatus lower the system pressure after the chamber back to 1 bar. A T-shape connector (2.9µL internal volume) was applied in front of the reactor. This mixer allowed the efficient mixing of the stock solutions prior entering the H-Cube reactor. In order to obtain information regarding reaction progress we integrated an FTIR flow cell for in-line analysis.[6] In comparison to other analytical techniques, FTIR spectroscopy is advantageous in that product formation can be continually analyzed in flow, avoiding delays due to sample extraction and subsequent analysis. Also, reaching the stationary state is determined directly. In addition to the hydrogenation apparatus and spectrometer, the reaction set up consisted of an HPLC pump, valve controls and an autosampler. The chosen Modified Simplex algorithm (MSIM)[4] was integrated in the programmed software, which centrally controlled the individual equipment components via RS-232 connections. The Simplex required reaction values from which improved reaction parameters (flow rate, temperature, pressure) can thus be calculated. In FTIR spectroscopy it is the peak height that is directly proportional to the reaction conversion and, via an auto-export function, this data is stored in a text file. This value is then read in real-time by the controlled optimization program. When the steady state (after a minimum of three hydrodynamic residence times and a standard deviation of $\leq 7 \cdot 10^{-4}$) of the system is reached the peak height is used as the measured value and, based on this result, the next set of parameters is calculated. In this manner completely autonomous self-optimization of the reaction parameters is possible.

After passing the in-line IR flow cell the valve controls the flow of a sample into the autosampler or collection vessels. As such all components and, thereby, the reaction parameters (flow rate, temperature and pressure) were controlled, regulated and optimized by the optimization software. The implemented MSIM-algorithm initially starts from an (n+1) shaped polygon in an n-dimensional parameter

space from which further optimization steps are derived. In our case three parameters (flow rate, temperature and H_2 pressure) give rise to four starting values.

Starting values were chosen within parameter ranges that formed a suitably large starting tetragon from which further optimization can be initiated (Table 1). The starting tetragon was created with one starting point *P1* and an edge length *c* based on a method of Spendley *et al.*.[5] All points which were generated by the MSIM-algorithm were rounded to the nearest step size value of the hydrogenation apparatus (flow rate in 0.1 $mLmin^{-1}$ steps, temperature in 5 K steps and pressure in 10 bar steps). This yielded a rather coarse grid. The hydrogenation system then drove the automated self-optimization in which the peak height of the isolated carbonyl band at 1704 cm^{-1}, directly proportional to the conversion, served as the value for the selection of the new parameter set. After 17 steps the reactor was able to autonomously determine the optimum conditions (Table 1, entry "*opt*"). Because the selectivity of the reaction approached unity at high conversions, the optimization with respect to conversion was also one with respect to yield.

IR-Cell data: Resolution: 4 cm^{-1} maximum; Optical Range (Base Unit): 4000 – 650 cm^{-1}; Cell: diamond.

Optimization of reaction conditions for benzaldehyde 1

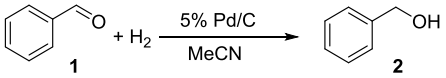

Closer inspection of Table S1 reveals that point 3 from the starting tetragon was revisited three times during optimization (13, 15, 17, indicated grey). This is likely with a coarse grid as in the present case. It does reveal an interesting feature of the Simplex routine: while the initial measurement only showed a conversion around 50%, it was consistently around 90% in the later runs. An initial transient, often due to a conditioning, is a characteristic feature of many heterogeneous catalytic systems.

The property of the Simplex algorithm to work only with the best (n+1) measurements and discard all others permits an optimum to be found even if it was initially not up to its steady-state value. The data further indicates that at the last three measurements shaded grey (i.e. at same conditions), the standard deviation of the IR data, which were the basis for the real-time optimization, was lower (2.7% relative) than that of the NMR data (3.9% relative).

Table S1 Starting parameter set (1-4, boxed) and subsequent runs for the hydrogenation of benzaldehyde **1**. Bold: Optimum run (14). Shaded: Repeated measurements at 800/85/30. c(benzaldehyde **1**) = 0.25 M, parameter limits for flow rate 0.3 – 1.0 $mLmin^{-1}$, temperature 20 – 100 °C, H_2 pressure 10 – 100 bar.

Entry		Flow rate [µL/min]	*T* [°C]	*p*(H_2) [bar]	IR peak height	Conversion by NMR
1	*start*	500	40	20	0,143(3)	15%
2	*start*	800	50	30	0,140(5)	17%
3	*start*	800	85	30	0,075(5)	54%
4	*start*	800	50	60	0,154(3)	10%
5		800	55	40	0,146(6)	12%
6		600	60	10	0,150(3)	8%
7		800	55	30	0,152(6)	8%
8		900	40	20	0,155(2)	11%
9		700	55	30	0,145(5)	13%
10		900	70	30	0,136(1)	18%
11		900	80	30	0,097(4)	48%

12		800	65	30	0,143(9)	18%
13		800	85	30	0,029(1)	94%
14	***opt***	**900**	**100**	**30**	**0,014(0)**	**95%**
15		800	85	30	0,030(6)	87%
16		800	75	30	0,112(5)	31%
17		800	85	30	0,030(4)	92%

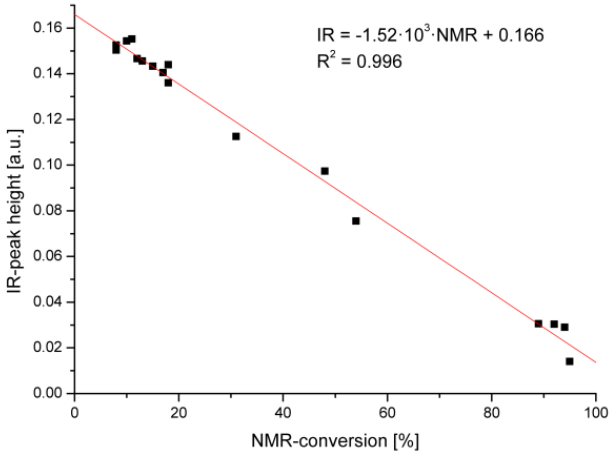

Figure S1 Linear correlation of IR peak height and NMR conversion of benzaldehyde **2.**

Optimization of reaction conditions for ketoester 3

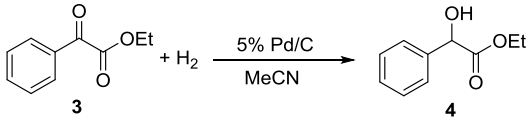

3 **4**

Table S2 Starting parameter set (1-4, boxed) and subsequent runs for the hydrogenation of ethylphenyl glyoxylate **3** to a-hydroxy ester **4.** Bold: Optimum run (10). Shaded: Runs with IR at its detection limit. c(ethylphenyl glyoxylate **3**) = 0.15 M, parameter limits for flow rate 0.3 – 1.0 mLmin^{-1}, temperature 20 – 75°C, H_2 pressure 10 – 100 bar.

Entry		Flow rate [µL/min]	*T* [°C]	*p*(H_2) [bar]	IR peak height	Conversion by NMR
1	*start*	700	30	10	0,038(2)	20%
2	*start*	1000	40	20	0,032(2)	32%
3	*start*	1000	75	20	0,022(0)	64%
4	*start*	1000	40	50	0,021(6)	51%
5		900	40	20	0,037(0)	24%
6		1000	45	30	0,028(3)	42%

7		1000	65	50	0,013(1)	85%
8		1000	75	50	0,013(5)	87%
9		1000	75	70	0,013(6)	98%
10	***opt***	**800**	**75**	**70**	**0,013(7)**	**99%**

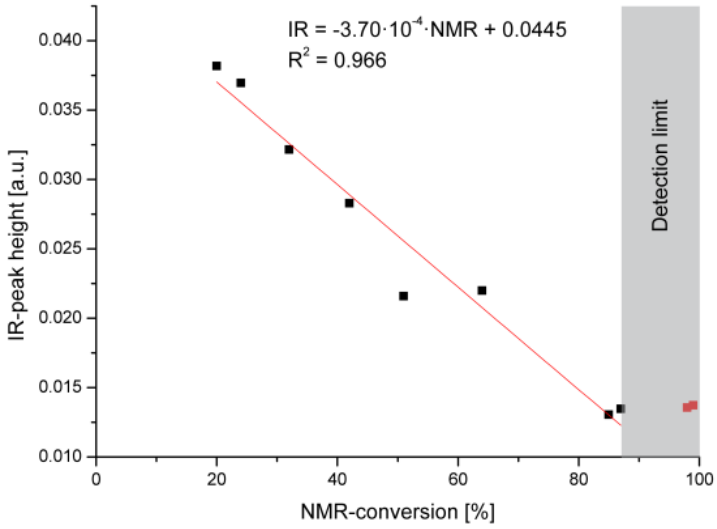

Figure S2 Linear correlation between IR peak height and NMR conversion. The red points illustrate that the detection limit for IR is reached. These points were not used for the linear regression.

An interesting observation is that from entry 7 on, the conversion of ≥85% was so high that the reactant signal in the IR spectrometer fell below the detection limit, due to the choice of spectral band (Figure 5). It can be seen that all subsequent measurements yielded the same IR peak height (Table 2, shaded area). In spite of this, the yield (as determined by off-line NMR) still increased. It can be shown that on an ascending slope in *n*-dimensional parameter space, the Simplex approach will continue for *n* steps beyond the point where the analytical method meets its detection limit.

The optimized points in both reactions were found at the maximum temperature for the system, respectively. It is likely that the conversion could even have increased at even higher temperature. For our objective, however, neither this nor the search of a global optimum was relevant. In addition to the temperature dependence, the pressure has a high influence on the conversion of the second hydrogenation, too. Among the possible reasons are hydrogen solubility issues, mass transfer limitations, or even a negative activation volume of the reaction.[7] The hydrogenation optimizations presented here take approx. 24 hours which in comparison to manual or automated sequential optimization is many times faster. For example, an automated sequential optimization (using 0.1 $mLmin^{-1}$, 5 K and 10 bar steps of 2 h each) which we described before[6] would take longer than three weeks. Hence, the newly developed, self-optimizing reactor system results in enormous time and cost savings which could not previously be achieved.

Optimization of reaction conditions for quinaldine 5

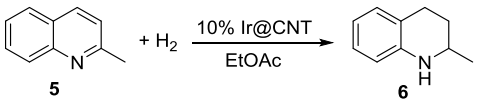

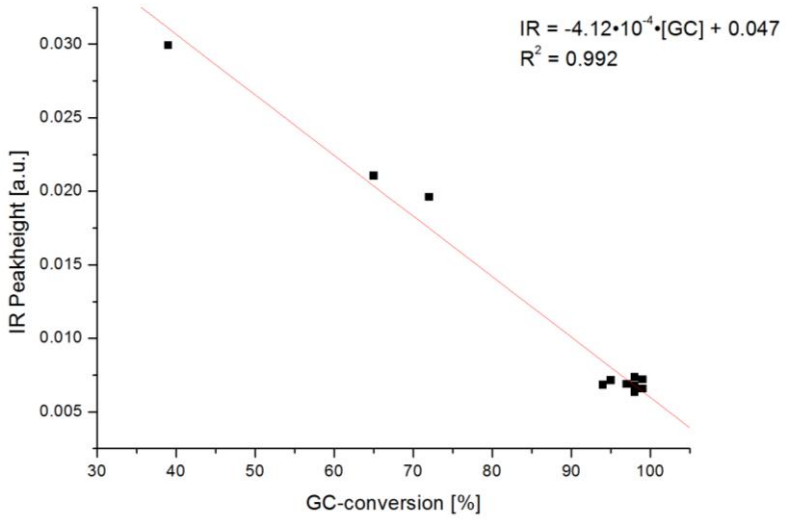

Figure S3 Linear correlation between IR peak height and NMR conversion.

In order to validate whether switches between high-pressure and low-pressure points have influences on the conversion in means of excessive hydrogen release onto the following parameter point, a 3-times cycle of five characteristically different set points were conducted (Figure S18+S19, Supporting Information). Seeing that all points give the same peak heights in the limits of accurateness, respectively, the system can be considered as being a reliable hydrogenation system.

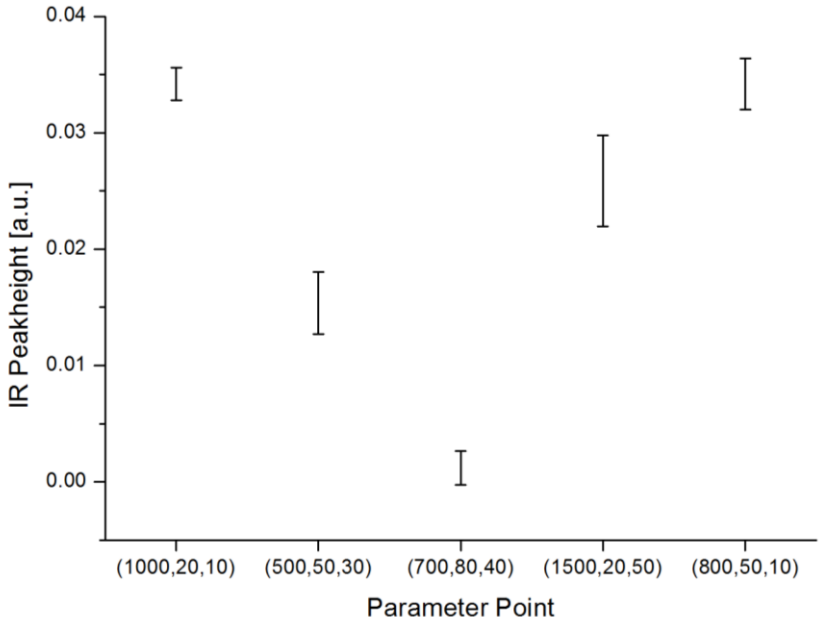

Figure S4 Control experiment performing a 3-times cycle of a 5-parameter switch (flowrate µLmin^{-1}, temperature °C, H_2-pressure bar) analyzed by IR peak height**.**

This was further confirmed when a five-times cycle of a 2-parameter switch between a high-pressure and low-pressure point was analysed (Figure S16+S17) showing stable conversions, respectively. Worth notably, an initial acclimatisation phase is required resulting from catalyst impregnations or adsorption by solvent and/or substrate. Nonetheless, this phenomenon intercepted during the optimisation process by the control algorithm as same parameters are reviewed again independently from its background.

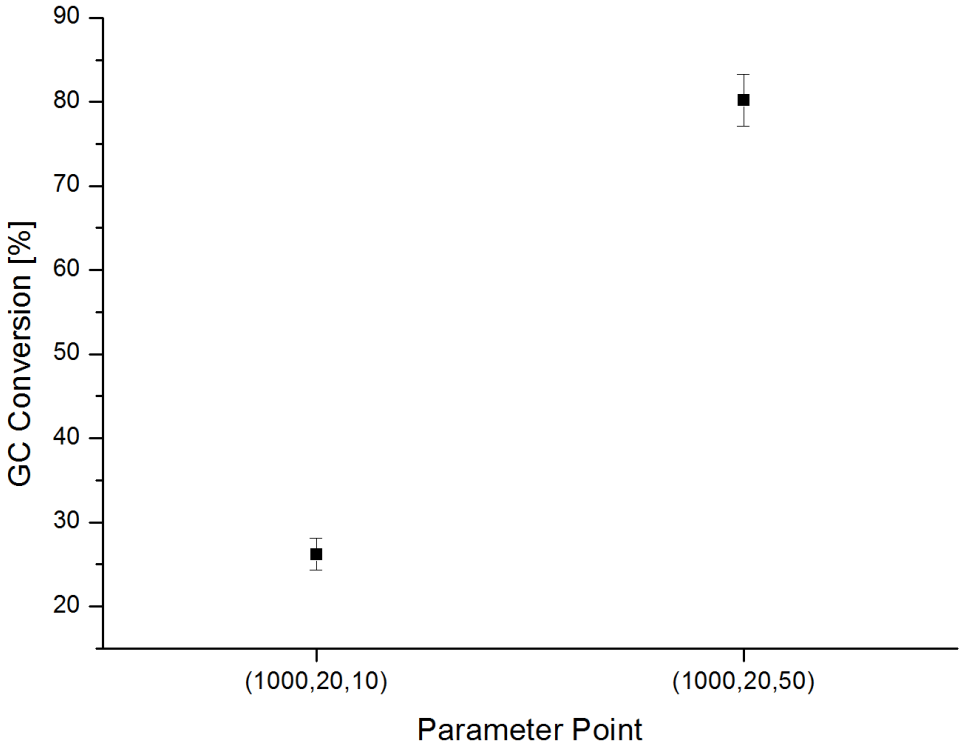

Figure S5 Control experiment performing a 5-times cycle of a 2-parameter switch (flowrate µLmin^{-1}, temperature °C, H_2-pressure bar) analyzed by GC**.**

Quinaldine Run 1(10 wt% Ir@CNT)

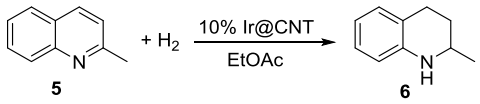

Table S3 Starting parameter set (1-4, boxed) and subsequent run **1** for the hydrogenation of quinaldine **5**. Shaded: Runs with IR at its detection limit.

Entry	Flow rate [µL/min]	*T* [°C]	*p*(H_2) [bar]	IR peak height	Conversion by GC
1 *Start*	700	40	10	0,029(9)	39%
2 *Start*	1000	50	20	0,019(6)	72%
3 *Start*	1000	85	20	0,021(1)	65%
4 *Start*	1000	50	50	0,0068(4)	94%
5	1300	85	50	0,0067(8)	98%
6	1200	40	60	0,0065(7)	99%
7	1100	55	40	0,0067(4)	98%
8	1400	70	50	0,0072(0)	99%
9	1100	55	50	0,0068(8)	97%
10	1300	85	50	0,0073(6)	98%
11	1200	50	50	0,0071(6)	95%
12	1100	30	50	0,0063(3)	98%

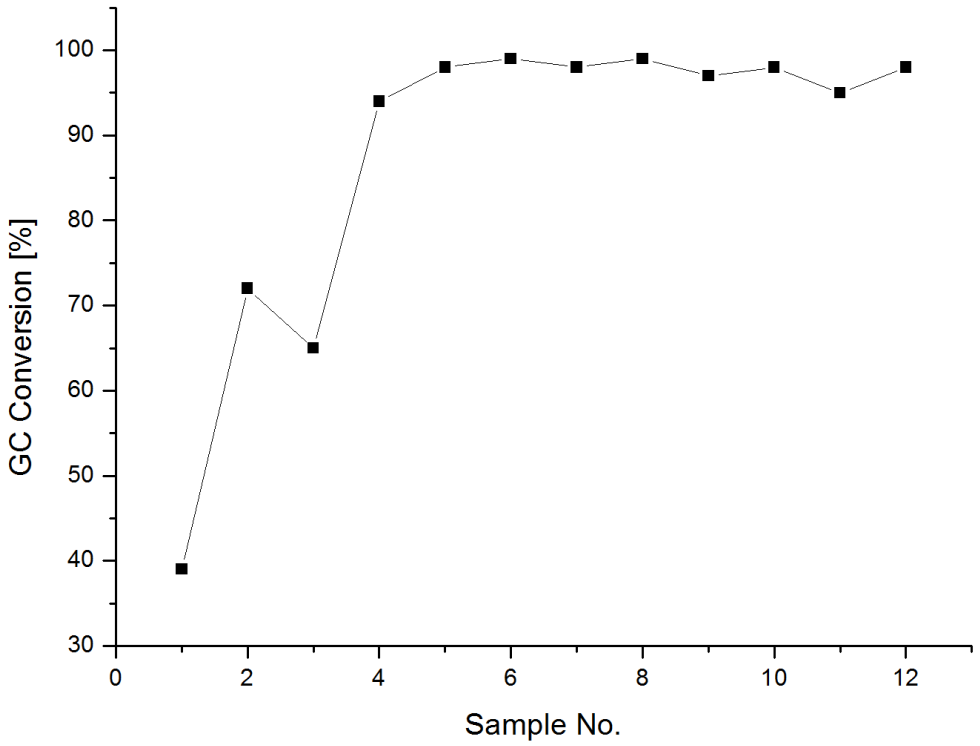

Figure S6 1st optimization run of quinaldine **5**.

Quinaldine Run 2 (10 wt% Ir@CNT)

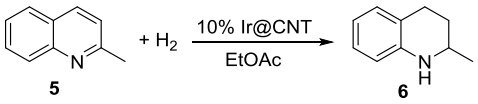

5 6

Table S4 Starting parameter set (1-4, boxed) and subsequent run 2 (reproduction) for the hydrogenation of quinaldine **5**. Shaded: Runs with IR at its detection limit.

Entry	Flow rate [µL/min]	*T* [°C]	*p*(H_2) [bar]	IR peak height	Conversion by GC
1 *Start*	700	40	10	0,023(6)	47%
2 *Start*	1000	50	20	0,014(1)	73%
3 *Start*	1000	85	20	0,014(6)	72%
4 *Start*	1000	50	50	0,0021(4)	94%
5	1300	85	50	0,0036(3)	97%
6	1200	40	60	0,0030(8)	99%
7	1100	55	40	0,0025(3)	99%
8	1200	65	50	0,0044(8)	98%
9	1000	75	30	0,0076(1)	95%
10	1200	40	60	0,0043(8)	99%
11	1000	30	50	0,0038(1)	99%

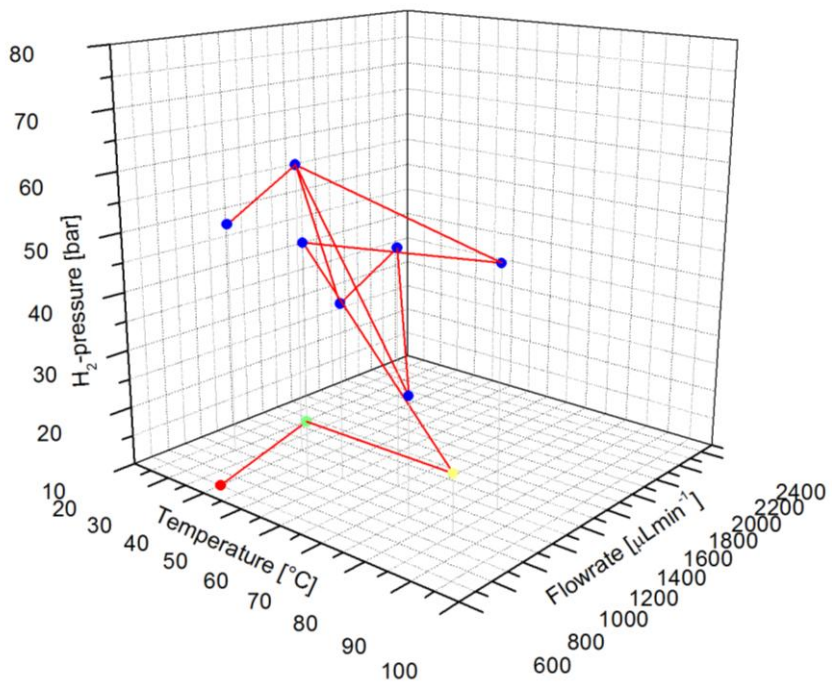

Figure S7 2nd optimization run of quinaldine **5** (4D-Plot).

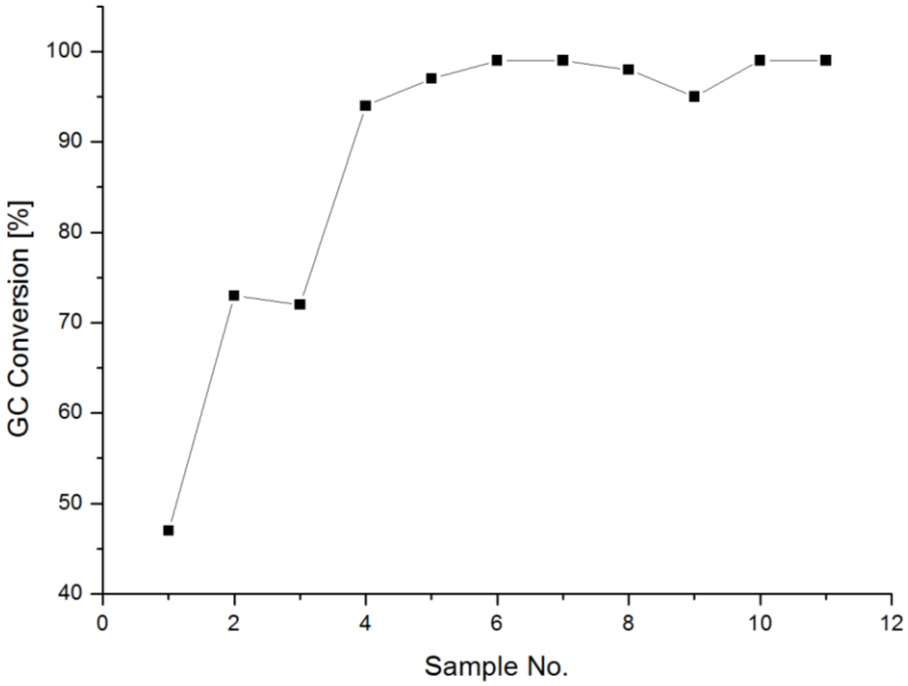

Figure S8 2nd optimization run of quinaldine **5** (sample-Plot).

Quinaldine Run 3 (10 wt% Ir@CNT)

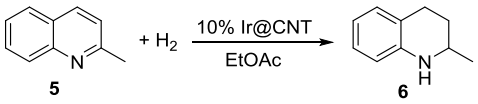

5 6

Table S5 Starting parameter set (1-4, boxed) and subsequent runs for the hydrogenation of quinaldine **5 (optimal starting conditions).** Shaded: Runs with IR at its detection limit.

Entry	Flow rate [µL/min]		*T* [°C]	*p*(H_2) [bar]	IR peak height	Conversion by GC
1	1500	1500	50	3.45E-4	90%
2	1800	1800	60	4.12E-4	94%
3	1800	1800	60	-1.96E-4	96%
4	1800	1800	70	-6.25E-4	98%
5	1600	1600	70	-5.11E-4	99%
6	1600	1600	60	-3.04E-4	98%
7	1700	1700	70	-5.83E-4	99%
8	1700	1700	70	-6.31E-4	99%
9	1900	1900	80	-4.42E-4	99%
10	1700	1700	70	-7.55E-4	99%
11	1800	1800	80	-3.37E-4	99%
12	1700	1700	70	-7.25E-4	99%

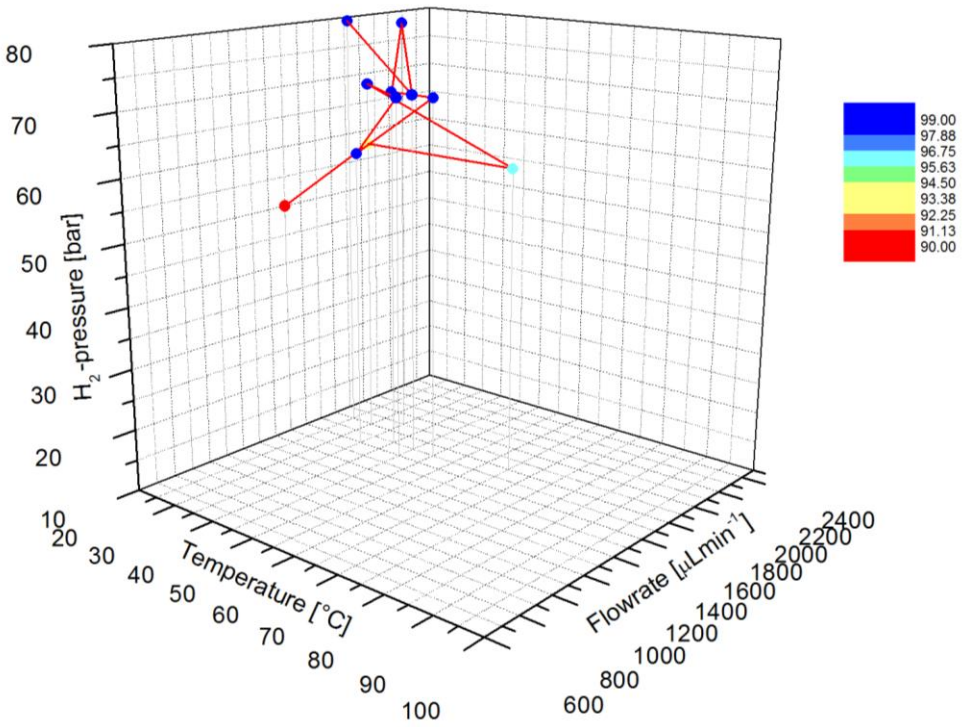

Figure S9 3nd optimization run of quinaldine **5** (4D-Plot).

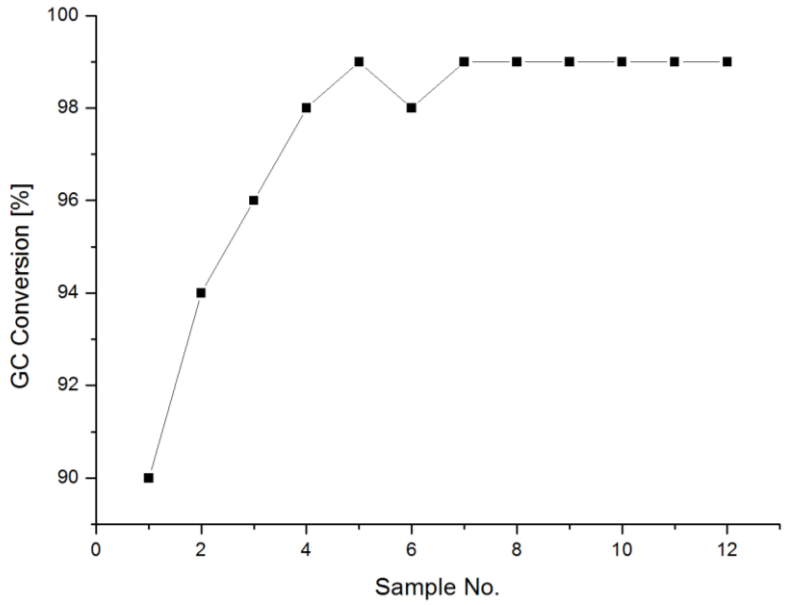

Figure S10 3nd optimization run of quinaldine **5** (sample-Plot).

Selectivity of Ir@CNT

The used Ir@CNT catalyst shows 100% selectivity for the hydrogenation of the heteroaromatic ring of quinaldine **5** over its benzene part. In order to verify this selectivity, 2-methyldecahydroquinoline was prepared using both Ir@CNT and Rh/C. The obtained compound was further analysed by FTIR spectroscopy using the ReactIR in EtOAc. Characteristic peaks (Fig. S21) for the entitled compound could not be found in previous collected spectra. Also when full conversion conditions were applied with high pressures and temperatures (60 bar, 80 °C, Fig. 22), only [H4]-quinaldine could be isolated and characterized by NMR spectroscopy.

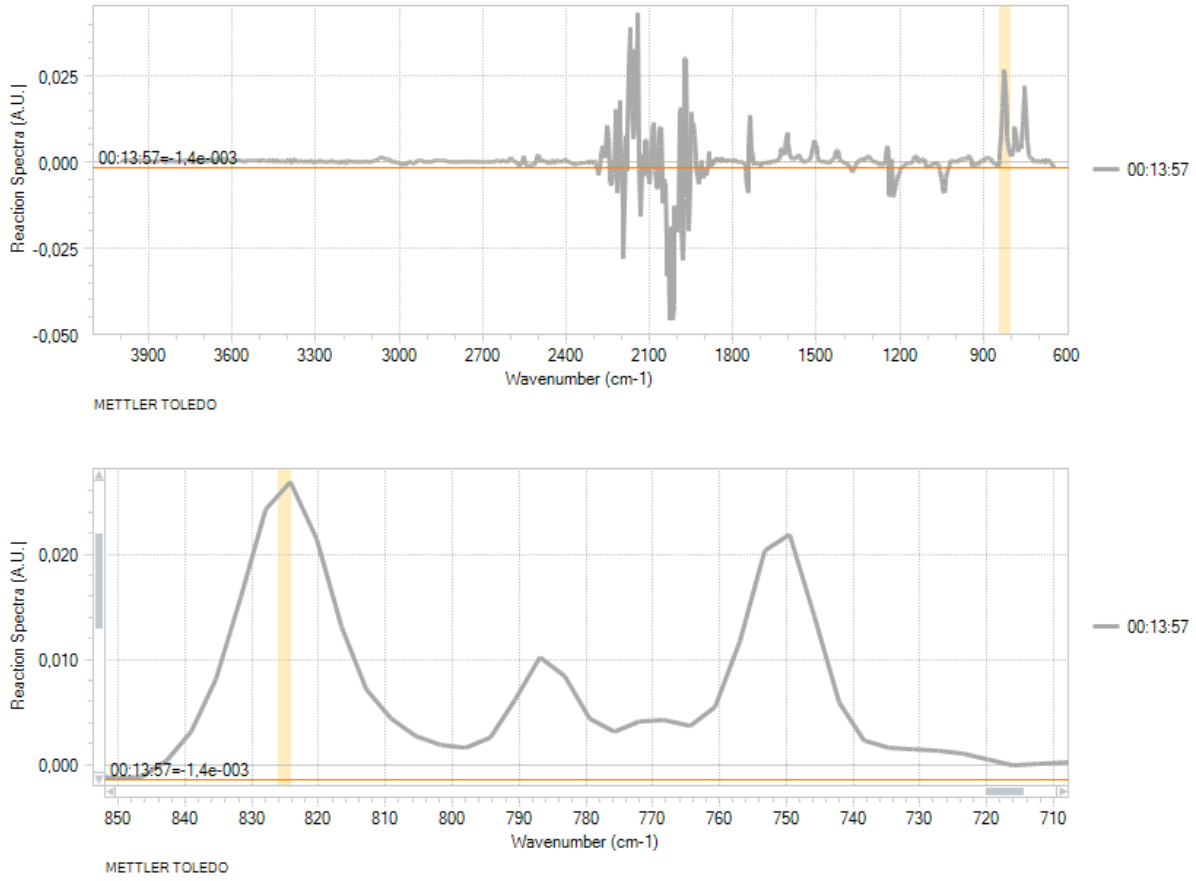

Figure S11 IR Spectra of quinaldine **5** in EtOAc (0.1 M), lower spectrum shows zoom in for characteristic band.

.

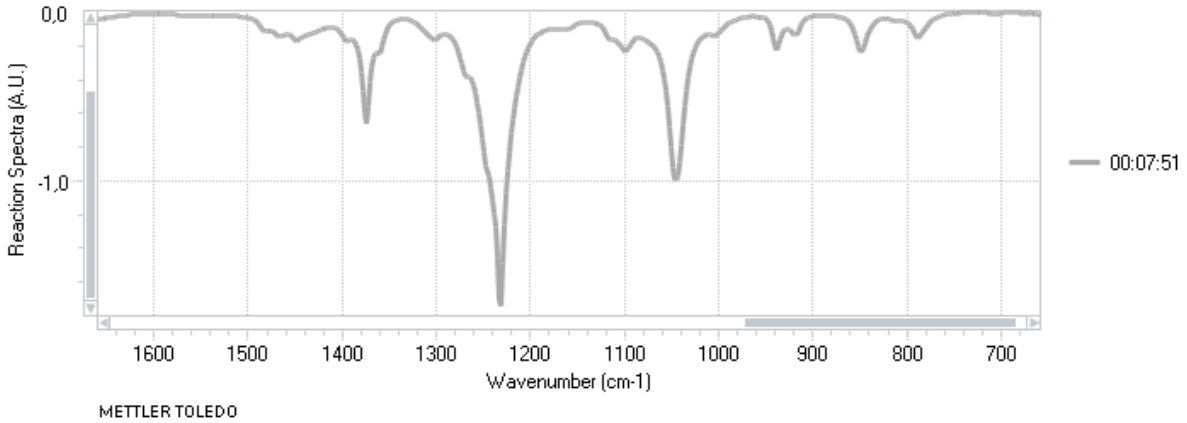

Figure S12 IR Spectra of 2-methyldecahydroquinoline in EtOAc.

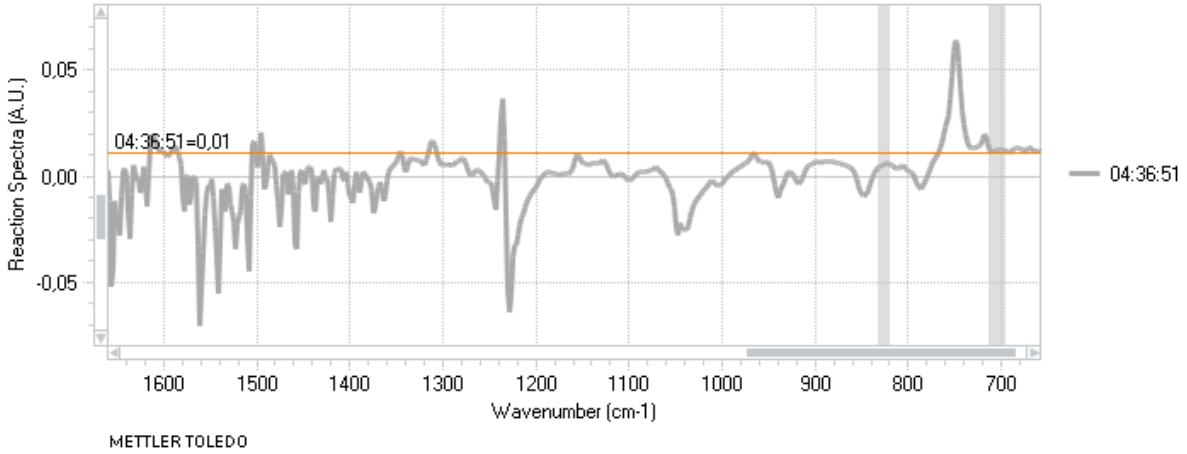

Figure S13 IR Spectra of quinaldine **5** in EtOAc (0.1 M) at point of full conversion (60 bar, 80 °C).

Optimization of reaction conditions for quinoxaline 7

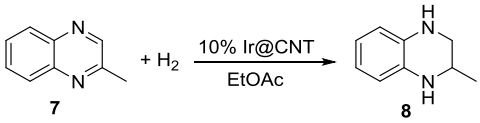

Table S6 Starting parameter set (1-4, boxed) and subsequent runs for the hydrogenation of quinoxaline **7.** Shaded: Runs with IR at its detection limit.

Entry		Flow rate [µL/min]	*T* [°C]	*p*(H_2) [bar]	IR peak height	Conversion by GC
1	*Start*	1000	20	10	0,016(4)	71%
2	*Start*	1500	30	20	0,023(4)	74%
3	*Start*	1500	65	20	0,023(2)	77%
4	*Start*	1500	30	50	0,0074(7)	99%
5		1300	45	30	0,0078(9)	98%
6		1400	50	30	0,0081(6)	98%
7		1600	65	60	0,0076(1)	99%
8		1500	45	60	0,0080(0)	98%
9		1500	45	60	0,0081(8)	97%
10		1300	45	30	0,0091(8)	97%

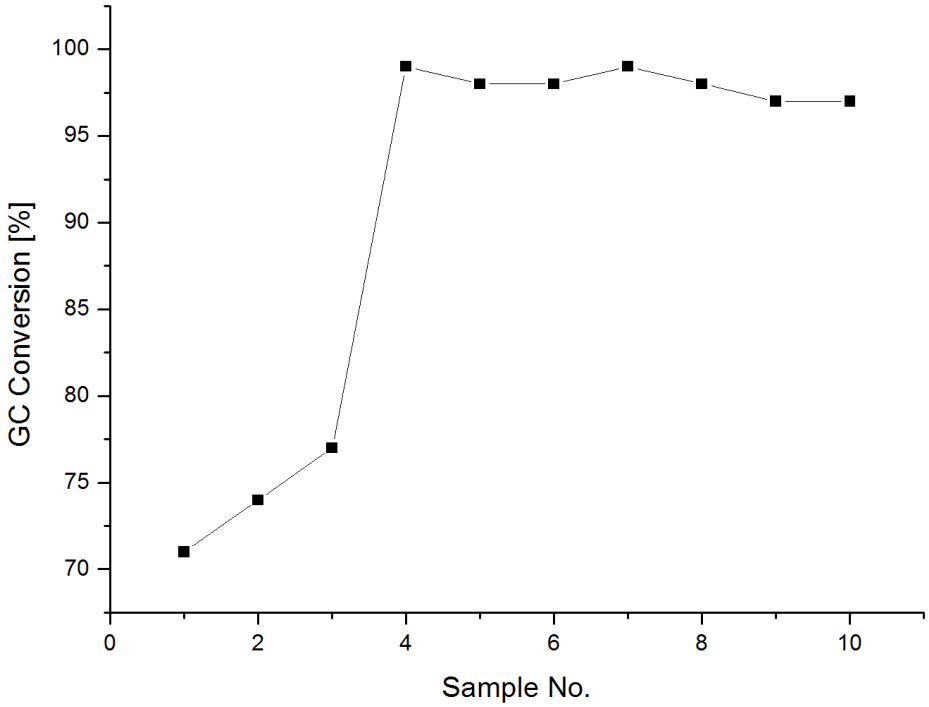

Figure S14 Optimization run of quinoxaline 7 (sample-Plot).

Quinaldine Adaptiv Run 1 (10 wt% Ir@CNT)

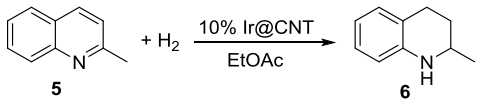

Table S7 Starting parameter set (1-4, boxed) and subsequent runs for the hydrogenation of quinaldine **5 (adaptive 1).**

Entry	Flow rate [µL/min]	*T* [°C]	*p*(H_2) [bar]	IR peak height	Conversion by GC
1	0,97581	50	10	0,9758(1)	50%
2	0,97847	79	20	0,9784(7)	79%
3	0,99604	92	20	0,9960(4)	92%
4	0,99732	96	50	0,9973(2)	96%
5	0,99683	98	50	0,9968(3)	98%
6	0,99811	100	60	0,9981(1)	100%
7	0,99641	95	40	0,9964(1)	95%
8	0,99634	95	50	0,9963(4)	95%
9	0,99548	96	60	0,9954(8)	96%
10	0,99628	92	50	0,9962(8)	92%
11	0,99622	96	50	0,9962(2)	96%
12	0,99199	99	60	0,9919(9)	99%
13	0,97938	39	50	0,9793(8)	39%
14	0,98947	96	60	0,9894(7)	96%
15	0,98374	92	60	0,9837(4)	92%
16	0,9697	39	50	0,9697(0)	39%
17	0,98404	87	60	0,9840(4)	87%
18	0,98617	84	50	0,9861(7)	84%
19	0,92785	52	60	0,9278(5)	52%
20	0,94056	61	50	0,9405(6)	61%
21	0,92529	95	60	0,9252(9)	95%
22	0,99348	93	60	0,9934(8)	93%
23	0,9911	95	50	0,9911(0)	95%
24	0,99284	98	50	0,9928(4)	98%

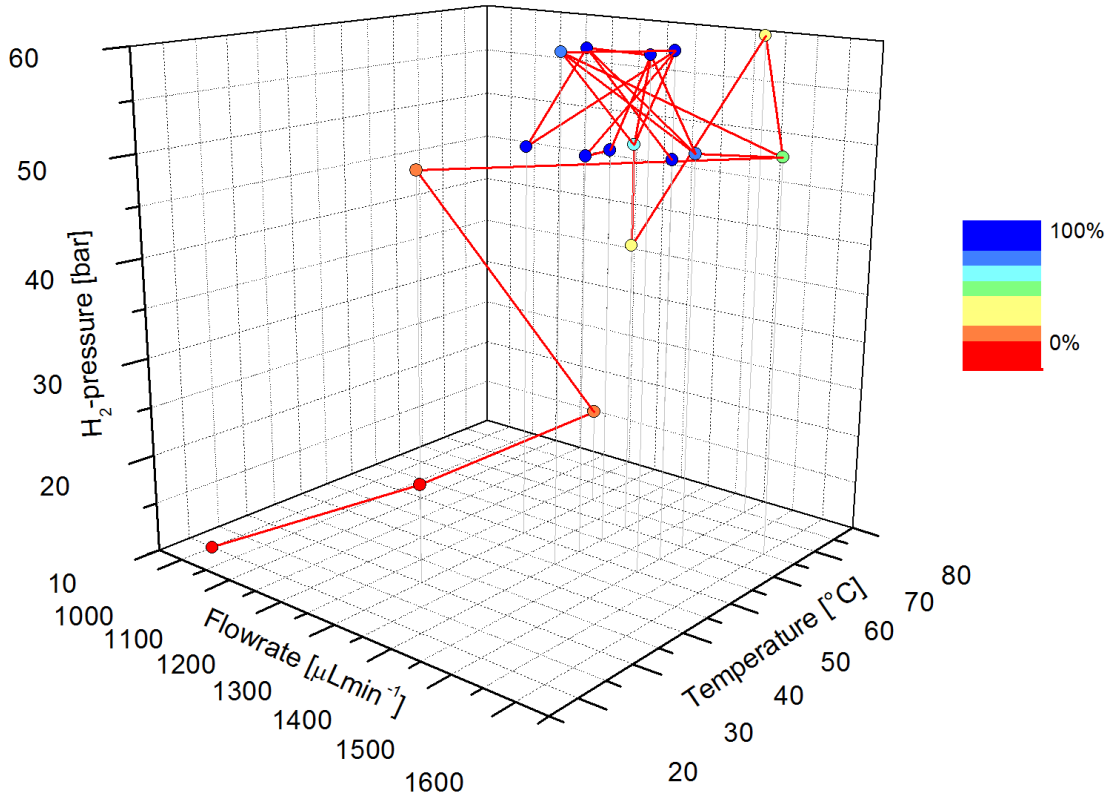

Figure S15 Adaptive optimization run 1 of quinaldine **5** (4D-Plot).

Quinaldine Adaptiv Run 2 (10 wt% Ir@CNT)

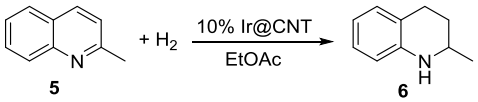

Table S8 Starting parameter set (1-4, boxed) and subsequent runs for the hydrogenation of quinaldine **5 (adaptive 2).**

Entry	Flow rate [µL/min]	*T* [°C]	*p*(H_2) [bar]	IR peak height	Conversion by GC
1	1000	20	10	0,9788(6	48%
2	1300	30	20	0,9975(4)	80%
3	1300	65	20	1,0021(3)	88%
4	1300	30	50	1,0041(3)	97%
5	1600	65	50	1,0057(8)	98%
6	1900	85	70	0,9719(8)	88%
7	1500	75	60	0,9898(2)	72%
8	1400	40	30	0,9554(5)	81%
9	1600	25	70	0,9146(2)	43%
10	1300	65	20	0,9427(7)	40%
11	1400	55	30	0,9508(3)	48%
12	1500	35	60	1,0039(3)	97%
13	1400	40	40	1,0018(0)	93%
14	1400	40	50	1,0017(0)	97%
15	1400	55	40	1,0010(7)	94%
16	1500	35	60	1,0005(6)	96%
17	1400	50	50	0,9999(7)	94%
18	1500	55	50	0,9995(1)	99%

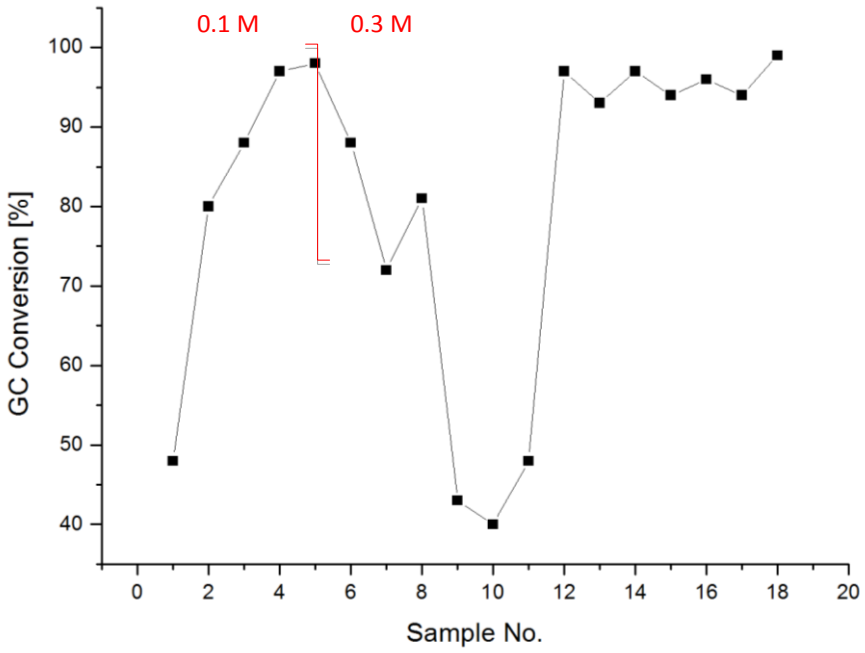

Figure S16 Adaptive optimization run 2 of quinaldine **5** (sample-Plot).

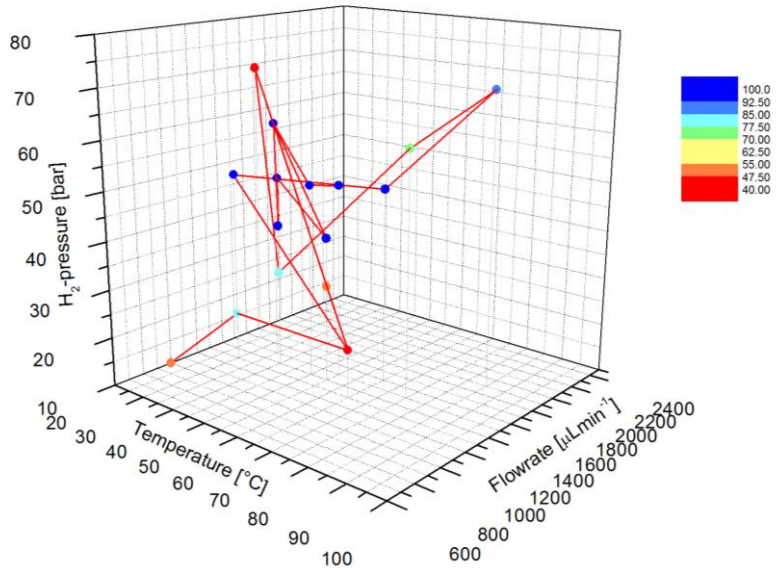

Figure S17 Adaptive optimization run 2 of quinaldine **5** (4D-Plot).

Quinaldine Adaptiv Run 3 (2.5 wt% Ir@CNT)

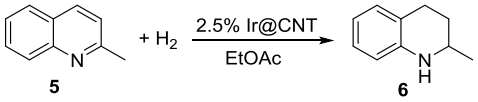

Table S9 Starting parameter set (1-4, boxed) and subsequent runs for the hydrogenation of quinaldine **5 (adaptive 3).**

Entry	Flow rate [µL/min]	*T* [°C]	*p*(H_2) [bar]	Conversion by GC
1	700	40	10	45
2	1000	50	20	89
3	1000	85	20	72
4	1000	50	50	91
5	1300	85	50	99
6	1200	40	60	98
7	1100	55	40	50
8	1100	85	30	41
9	1200	40	60	73
10	1100	55	50	67
11	1100	85	40	60
12	1200	50	60	75
13	1200	60	60	81
14	110	85	50	76
15	1200	80	50	75
16	1100	75	40	62
17	1200	70	60	85
18	110	55	60	80
19	1200	60	60	84
20	1100	60	50	83
21	1200	65	50	82
22	1100	75	40	71
23	1200	60	60	93
24	1100	65	60	97

25	1100	75	50	86
26	1200	65	60	90
27	1200	70	50	84
28	1100	65	60	89
29	1200	65	60	91
30	1100	70	50	84
31	1200	65	60	92

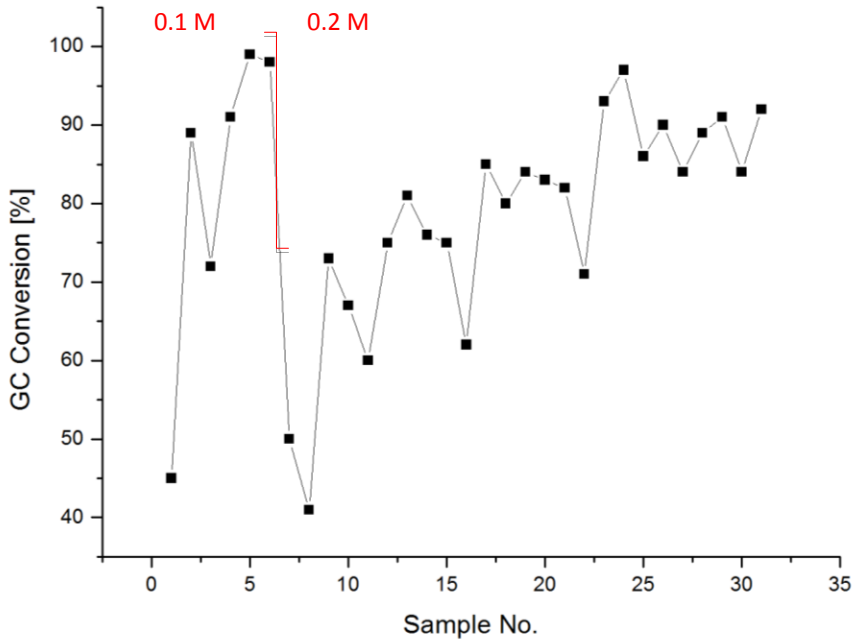

Figure S18 Adaptive optimization run 3 of quinaldine **5** (sample-Plot).

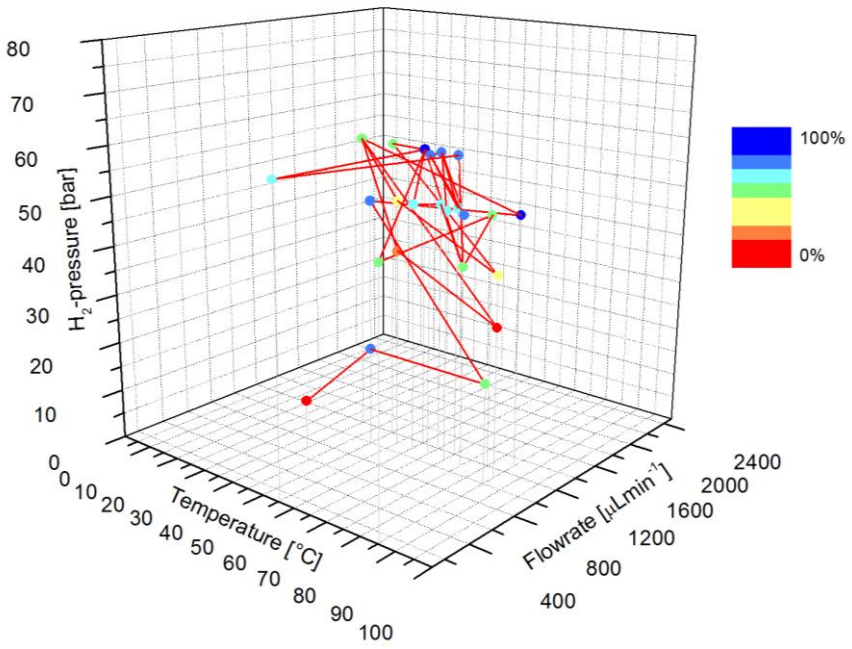

Figure S19 Adaptive optimization run 3 of quinaldine **5** (4D-Plot).

NMR Data

Benzyl alcohol

1H-NMR ($CDCl_3$): 7.50-7.24 (m, 5H), 4.61 (s, 3H), 3.7 (bs, 1H) ppm.

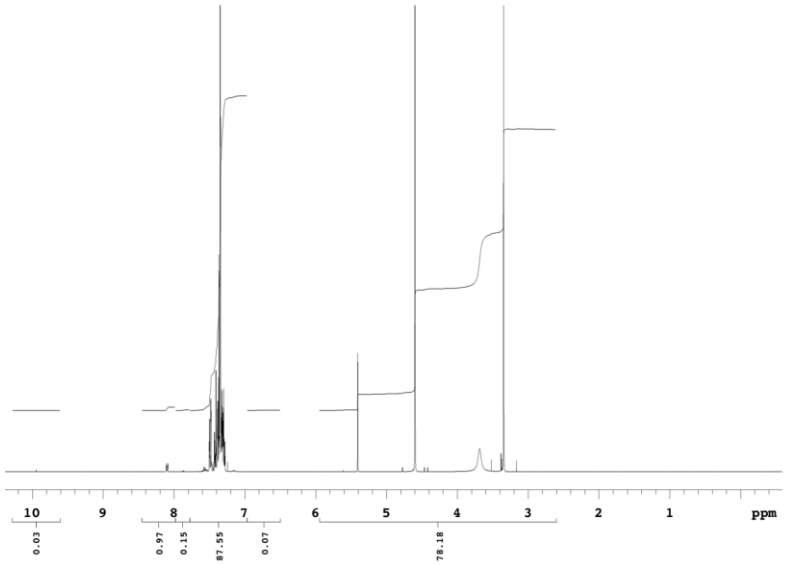

1 http://www2.knauer.net/e/e_index.html?cf=%27http://www2.knauer.net/cgi-bin/e_prodpage.pl?artnr=A41509&zusatz=10%20ml%20pump%20head%2C%20inert%2C%20with%20titanium%20inlays&ptype=Pumps%27
2 http://www.hitec-zang.de/de/liquid-handlinglaborroboter/automatischer-probensammler.html
3 http://webstore.idex-hs.com/
4 E. Morgan, K. W. Burton, and G. Nickless, *Chemom. Intell. Lab. Syst.*, 1990, **7**, 209-222.
5 W. Spendley, G. R. Hext, and F. R. Himsworth, *Technometric*, 1962, **4**, 441-461.
6 Articles on flow FTIR: a) T. Brodmann, K. Koos,. A. Metzger, P. Knochel, and S. V. Ley, *Org. Process Res. Dev.*, 2012, **16**, 1102-1113; b) J. Keybl, and K. F. Jensen, *Ind. Eng. Chem. Res.*, 2011, **50**, 11013-11022.
7 F. Benito-Lopez, W. Verboom, M. Kakuta, J. G. E. Gardeniers, R. J. M. Oosterbroek, A. van den Berg, and D. N. Reinhoudt, *Chem. Commun.*, 2005, 2857-2859.